

IPC2016-64553

## EFFECT OF RESIDUAL FORMING STRESSES ON FRACTURE IN ERW PIPE

**Ted L. Anderson**  
Team Industrial Services, Inc.  
Boulder, Colorado, USA

**Gregory W. Brown**  
Quest Integrity Group  
Boulder, Colorado, USA

### ABSTRACT

Many older pipelines contain significant residual stress due to the forming process. Cold expansion or a normalizing heat treatment can virtually eliminate residual forming stresses, but these practices were less common in the past. In the absence of cold expansion or normalization, residual forming stresses can be *reduced* by hydrostatic testing or operating pressures, but not eliminated entirely. Residual stresses can contribute to fracture in pipelines, particularly when the material toughness is low.

This article presents a series of analyses that seek to quantify the magnitude of residual forming stresses as well as their impact on pipeline integrity. The pipe forming process was simulated with elastic-plastic finite element analyses, which considered the effect of subsequent loading on relaxation of residual stresses. A second set of finite element simulations were used to quantify the effect of residual stresses on fracture behavior.

### BACKGROUND

When ERW pipe is formed from steel plate, yield-magnitude residual stress may develop in the pipe body. These residual stresses can be virtually eliminated through cold expansion or a normalizing heat treatment. In the absence of cold expansion or normalization, residual forming stresses can be *reduced* by hydrostatic testing or operating pressures, but not eliminated entirely. Vintage ERW pipelines with sparse or non-existing hydrostatic test records may contain significant residual forming stresses. When a pipe joint with residual forming stresses unzips along the seam in service or during a pressure test, there is often a measureable spring-back, where the matching halves of the fracture surface are separated by several inches. The ASTM standard E1928 (1) includes a formula for calculating residual forming stresses from the measured spring-back. Spring-back is a common occurrence when vintage ERW pipe joints fail, which is clear evidence that residual forming

stresses are real. However, fracture models traditionally employed by the pipeline industry fail to incorporate the effect of residual stresses.

The authors have performed a series of finite element analyses to simulate the ERW manufacturing process. These analyses also consider post-forming events, including cold expansion, hydrostatic testing, and fracture. For pipes that are not cold expanded, the effect of maximum pressure on residual stress relief was quantified.

Residual forming stresses can contribute to fracture of vintage pipe joints with low toughness. A number of in-service failures have occurred at very low operating pressures. Given realistic toughness properties for carbon steel, hoop stresses from pressure alone were not sufficient to explain the observed failures. An additional source of loading must have contributed to the failures, and residual forming stresses are the most likely culprit. In the present article, the effect of residual stresses on burst pressure is demonstrated using the PRCI MAT-8 model (2).

### FINITE ELEMENT SIMULATION OF PIPE FORMING

Figure 1 shows images from a finite element simulation of pipe forming. The analysis considered a 20-inch diameter pipe with 0.312-inch wall. An elastic-plastic material model was incorporated into the analysis, with yield and tensile strength values corresponding to specified minimum properties for the API 5L-X60 grade. The pipe was idealized with a half-symmetric 2D plane strain assumption. The Abaqus commercial finite element software was used for all simulations. An initially flat steel plate was formed around a rigid mandrel, as Fig. 1 illustrates. The ERW seam was simulated by imposing a constraint on the model at the 12 o'clock position. The heat from welding was also applied at the seam. Multiple load cases considered post-forming events such as cold expansion and hydrostatic testing.

Figure 2 is a plot of the through-wall distribution of residual hoop stresses for various load cases. Yield-magnitude residual stresses are created immediately after welding. Subsequent loading relieves residual stresses to varying degrees. Cold expansion by 1.5% or a hydrostatic test to 125% of yield effectively removes residual stresses. In the absence of a cold expansion treatment, the magnitude of residual stresses in the pipe body is a function of the maximum pressure the pipe has seen in its lifetime.

Residual forming stresses are compressive on the ID of the pipe and tensile on the OD due to bending during the manufacturing process (Fig. 1). Thus the through-wall hoop stress distribution is predominately bending. Figure 3 is a plot of linearized residual stresses, which corresponds to the equivalent through-wall bending moment.

When a pipe joint fails at the ERW seam, it may spring open. This spring-back effect is a manifestation of residual forming stresses. The ASTM standard E1928 contains the following equation to calculate the residual forming stresses from the magnitude of the spring-back:

$$\sigma_b^R = \frac{Et}{1-\nu^2} \left( \frac{1}{D_o} - \frac{1}{D_i} \right) \quad [1]$$

where  $\sigma_b^R$  is the linearized residual bending stress,  $E$  is Young's modulus,  $t$  is wall thickness,  $\nu$  is Poisson's ratio,  $D_o$  is the initial pipe diameter and  $D_i$  is the diameter after spring-back. This equation has been used in conjunction with destructive testing on new pipe joints to quantify residual stresses that result from a particular fabrication procedure. Equation [1] can also be applied to a seam weld failure that occurs in service or during a pressure test. Whether a cut is intentionally made in a pipe joint or the pipe unzips, the spring-back can be used to infer the residual forming stresses in the pipe body.

The finite element simulations were benchmarked to Eq. [1] by releasing the constraints at the seam and allowing the pipe model to spring open. The results of this exercise are plotted in Fig. 4, which shows good agreement between the FEA models and Eq. [1].

## EFFECT OF RESIDUAL STRESSES ON FRACTURE

It is a well established fact that residual stresses contribute to crack driving force, which controls fracture. When loading is purely elastic, stresses from various sources (e.g. hoop stress from pressure versus residual stress) impact the structure in an identical manner. When plastic deformation occurs, primary loads such as pressure behave differently from residual stresses, but both contribute to fracture. Pressure stresses are load-controlled, so they persist into the plastic range. Residual stresses relax with plastic deformation, however.

The pipeline industry has largely ignored the effect of residual forming stresses on fracture. Fracture models that the industry has traditionally used, including Log Secant and CorLAS, account only for hoop stress from pressure.

Although modern manufacturing processes such as UOE have largely eliminated the issue in new construction, there is no question that many vintage pipelines have significant residual forming stresses. There is ample indirect evidence for the impact of residual stresses on fracture, as a number of in-service failures have occurred at very low pressures. The implication is that another source of loading must have been present, and residual stresses is the most likely suspect. There is also significant direct evidence in the form of spring-back following many seam weld failure. While one may argue that failures at low pressures are due to extremely poor material properties, the spring-back effect is unequivocal proof of the release of residual stresses upon failure.

Although traditional pipeline fracture models do not account for residual forming stresses, modern models based on sound fracture mechanics principles incorporate all forms of stress. For example, the failure assessment diagram (FAD) model in API 579 (3) is capable of including residual stresses. The PRCI MAT-8 fracture model (2) is based on fits to elastic-plastic finite element solutions for pipes with longitudinal cracks. The original publication of the MAT-8 model did not consider residual stresses, but recent work presented below rectifies that situation.

The PRCI MAT-8 model quantifies crack driving force with the J-integral. Elastic-plastic finite element solutions for pipes with axial cracks were fit to the following expression:

$$J = J_{el} \left[ 1 + L_r^{n-1} + \frac{\beta L_r^2}{1 + L_r^{n-1}} \right] \quad [2]$$

where  $J_{el}$  is the elastic J-integral solution,  $L_r$  is the load ratio, which is a dimensionless function of the hoop stress and crack dimensions,  $\beta$  is a fitting parameter and  $n$  is a strain hardening exponent. It is often convenient to express the J-integral as an equivalent stress intensity factor:

$$K_J = \sqrt{\frac{JE}{1-\nu^2}} \quad [3]$$

Equations [2] and [3] consider only pressure loading. Residual stresses can be incorporated by summing the contributions from primary and residual stresses to crack driving force:

$$K_J^{tot} = K_J^P + VK_J^R \quad [4]$$

where  $K_I^p$  is the elastic-plastic crack driving force due to primary loads such as pressure,  $K_I^R$  is the elastic stress intensity factor due to residual stresses, and  $V$  is a plasticity correction. For a semi-elliptical surface crack,  $K_I^R$  is given by

$$K_I^R = \sigma_b^R G_b \sqrt{\frac{\pi a}{Q}} \quad [5]$$

Where  $G_b$  is a geometry factor,  $a$  is the crack depth, and  $Q$  is a flaw shape parameter.

A series of 3D elastic-plastic finite element simulations have recently been performed to supplement the original PRCI MAT-8 project described in Ref. (2). As with the original work scope, the new analyses considered pipes with longitudinal axial cracks. Residual bending stresses were achieved by imposing a through-wall temperature gradient on the FEA model. The magnitude of the through-wall bending stress,  $\sigma_b^R$ , is proportional to the imposed temperature gradient. The resulting  $K_I$  solutions with and without residual stresses were compared in order to infer  $V$  in Eq. [4], which is the plasticity correction on  $K_I^R$ . The following expression was fit to the aforementioned finite element results:

$$V = \frac{1 + \rho L_r^3}{1 + L_r^{2n}} \quad [6]$$

where

$$\rho = \begin{cases} \frac{0.2567}{G_b} \left( \frac{\sigma_b^R}{\sigma_{YS}} \right)^{-0.852} & (\sigma_b^R / \sigma_{YS}) \geq 0.1 \\ \frac{1.826}{G_b} & (\sigma_b^R / \sigma_{YS}) < 0.1 \end{cases} \quad [7]$$

Figure 5 is a plot of  $V$  versus load ratio,  $L_r$ . In the linear elastic range (i.e. as pressure  $\rightarrow 0$ ), the stress intensity factors due to pressure loading and residual stress are additive, so  $V = 1$ . As pressure increases,  $V > 1$  due to plastic zone effects. Mechanical stress relief occurs in the fully plastic regime, and  $V \rightarrow 0$ .

The above equations apply to surface cracks on the OD surface, where residual stresses are positive. For cracks on the ID surface, residual stresses can be ignored.

The effect of residual stresses on fracture can be demonstrated by applying the modified PRCI MAT-8 model to a collection of seam weld failures that occurred in service or during hydrostatic testing. These failures are documented in

two reports to PHMSA (4, 5), which were part of a large study on seam weld integrity. Given the pipe dimensions, crack dimensions, burst pressure and tensile properties, the fracture toughness of the seam weld (i.e., the critical  $J$  at failure) can be inferred from the modified PRCI MAT-8 model presented above. In other words, each documented burst event can be treated like a  $J$  test on the seam. In 124 cases, the aforementioned PHMSA reports contain sufficient information to infer fracture toughness at seam welds that failed.

Figure 6 is a cumulative probability plot of inferred fracture toughness from the 124 burst events. The assumed residual stresses were varied from zero to 60% of the actual yield strength of the individual pipe joints that failed. The lowest inferred toughness values were observed for several failures that resulted from selective seam corrosion. In the worst case, the burst pressure was only 20% of SMYS, which implied a fracture toughness of approximately 6 ksi $\sqrt{\text{in}}$  if residual stresses are disregarded. Such a low toughness is unrealistic for carbon steel, but more reasonable inferred toughness values are obtained when residual stresses are included in the analysis.

Note that at inferred toughness values greater than 90 ksi $\sqrt{\text{in}}$ , the shape of the data trend in Fig. 6 changes and the assumed residual stresses have little or no effect on the analysis. The set of seam weld failures documented in the PHMSA reports included cases where burst was preceded by significant plastic deformation. Referring to Eq. [4] and Fig. 5, plastic deformation at high pressures (relative to yield) results in mechanical stress relief, where residual stresses relax. Mechanical stress relief effects are also evident in Figs. 2 and 3.

The abrupt change in slope in the cumulative probability versus inferred toughness data in Fig. 6 reflects a transition from *toughness-controlled failure* to *collapse-controlled failure*. Figure 7 is a schematic plot of burst pressure versus toughness for a given crack size. The burst pressure is sensitive to toughness for low-toughness materials, but burst pressure reaches a plateau at high toughness. Once the toughness is sufficiently high, further increases in toughness have diminishing returns because burst is controlled by strength properties. In the collapse-controlled regime, a crack results in essentially the same burst pressure as a metal loss flaw with the same length and depth. In the toughness-controlled regime, the material is *notch sensitive* and sharp planar cracks can exhibit significantly lower failure pressures than metal loss flaws. Residual stresses play an important role in the toughness-controlled regime.

## CONCLUDING REMARKS

The existence of significant residual forming stresses in some seam-welded pipelines is incontrovertible. The creation of residual stresses during traditional pipe forming practices is simply a matter of physics. The spring-back (or spring-open) that often accompanies seam weld failures is direct proof of the presence of forming stresses, even after many years of operation.

Residual forming stresses are important to the integrity of the pipeline when three conditions are met:

1. The material toughness in the seam is low.
2. One or more surface-breaking cracks are present on the OD of the pipe.
3. The pipe was not cold expanded or normalized at the time of manufacture.

We can disregard residual stresses for ID cracks, blunt notch-like flaws, metal loss flaws, and for high-toughness materials. Moreover, modern manufacturing processes such as cold expansion and normalizing have largely eliminated the problem for newer pipelines.

For situations where residual stresses play a potential role, one must use modern fracture mechanics models that are capable of incorporating residual stress effects. Fracture models that have traditionally been used in the pipeline industry, which are not capable of incorporating residual stress, must be discarded in favor of more robust methods.

Perhaps the primary reason why the impact of residual forming stresses on pipeline integrity has not been considered previously is that the magnitude of residual stresses in a given pipeline is largely unknown. Modern finite element techniques, such as those employed in this study, can be used to estimate residual stresses, given a knowledge of fabrication procedures and the hydrostatic testing history. Moreover, recent PHMSA-sponsored research resulted in nondestructive examination (NDE) technology that is capable of in-the-ditch residual stress measurements.

In cases where the manufacturing process and hydro test history of a pipeline is unknown, an assumed residual stress of 50% SMYS can be used in a fracture analysis. This assumption will be conservative in most instances.

## NOMENCLATURE

$a$  – Crack depth.

$D_1$  – Diameter after spring-back from residual stress.

$D_o$  – Diameter before failure.

$E$  – Young's modulus.

$G_b$  – Elastic stress intensity geometry factor.

$J$  – J-integral.

$J_{el}$  – Elastic component of  $J$ .

$K_I^R$  – Elastic stress intensity due to residual stress.

$K_J$  – Stress intensity factor computed from  $J$ .

$K_J^P$  – Crack driving force due to primary stress.

$L_r$  – Load ratio.

$Q$  – Flaw shape parameter.

$t$  – Pipe wall thickness.

$V$  – Plasticity correction factor on  $K_I^R$ .

$\beta$  – Fitting parameter for J-integral solutions.

$\nu$  – Poisson's ratio.

$\rho$  – Fitting parameter for  $V$ .

$\sigma_b^R$  – Residual bending stress.

$\sigma_{ys}$  – Yield strength.

## ACKNOWLEDGMENTS

The authors wish to acknowledge the support of ExxonMobil Research and Engineering.

## REFERENCES

1. E1928-13, "Standard Practice for Estimating the Approximate Residual Circumferential Stress in Straight Thin-walled Tubing." American Society for Testing and Materials, Philadelphia, PA, 2013.
2. Anderson, T.L., "Development of a Modern Assessment Method for Longitudinal Seam Weld Cracks." Pipeline Research Council Inc., Catalog No. PR-460-134401, 2016.
3. API 579-1/ASME FFS-1, *Fitness-for-Service*, jointly published by the American Petroleum Institute and the American Society for Mechanical Engineers, June 2007.
4. Kiefner, J.F. and Kolovich, K.M., "ERW and Flash Weld Seam Failures." Final Report as the Deliverable of Sub-Task 1.4 on U.S. Department of Transportation Other Transaction Agreement No. DTPH56-11-T-000003, September 24, 2012.
5. Kiefner, J.F. and Kolovich, K.M., "Models for Predicting Failure Stress Levels for Defects Affecting ERW and Flash-Weld Seams." Final Report as the Deliverable of Sub-Task 2.4 on U.S. Department of Transportation Other Transaction Agreement No. DTPH56-11-T-000003, January 3, 2013.

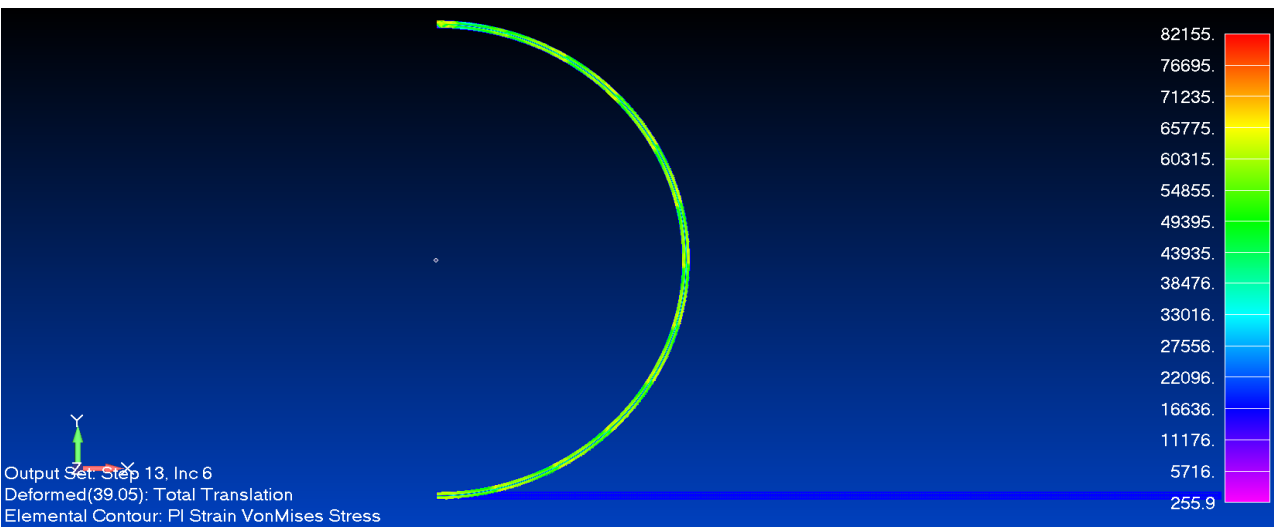
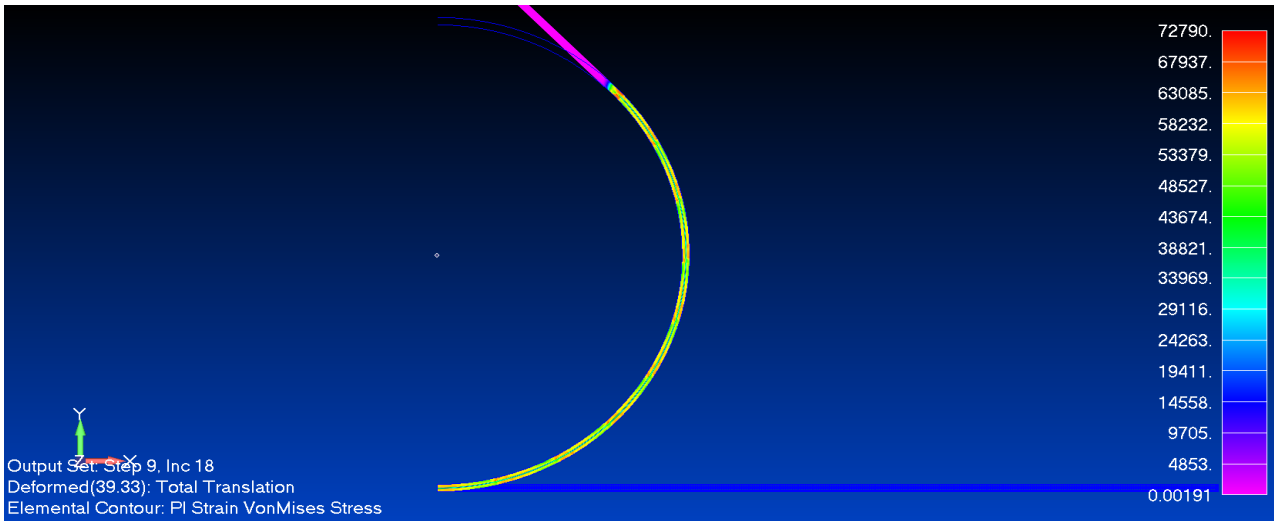
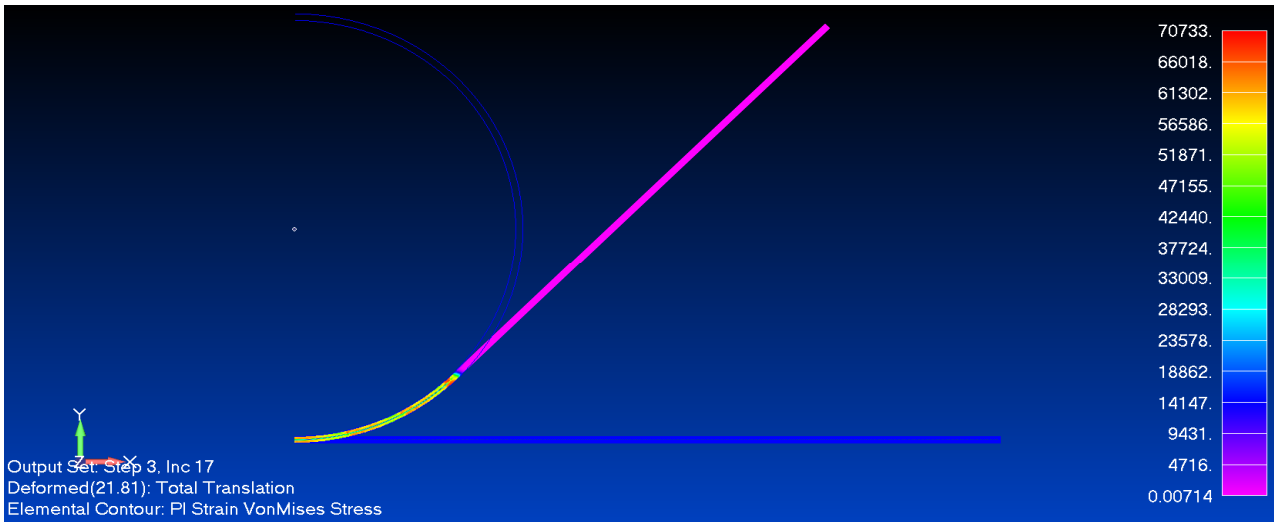


FIGURE 1. Elastic-plastic finite element simulation of forming ERW pipe.

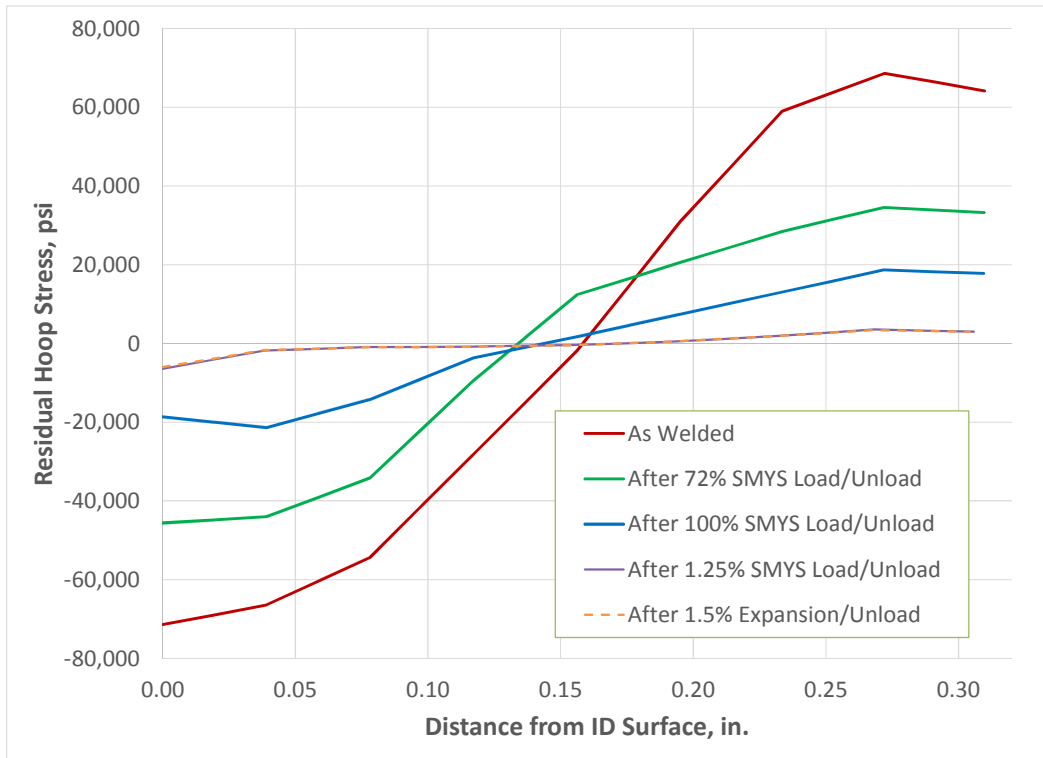


FIGURE 2. Through-wall variation of residual hoop stress due to pipe forming and subsequent loading.

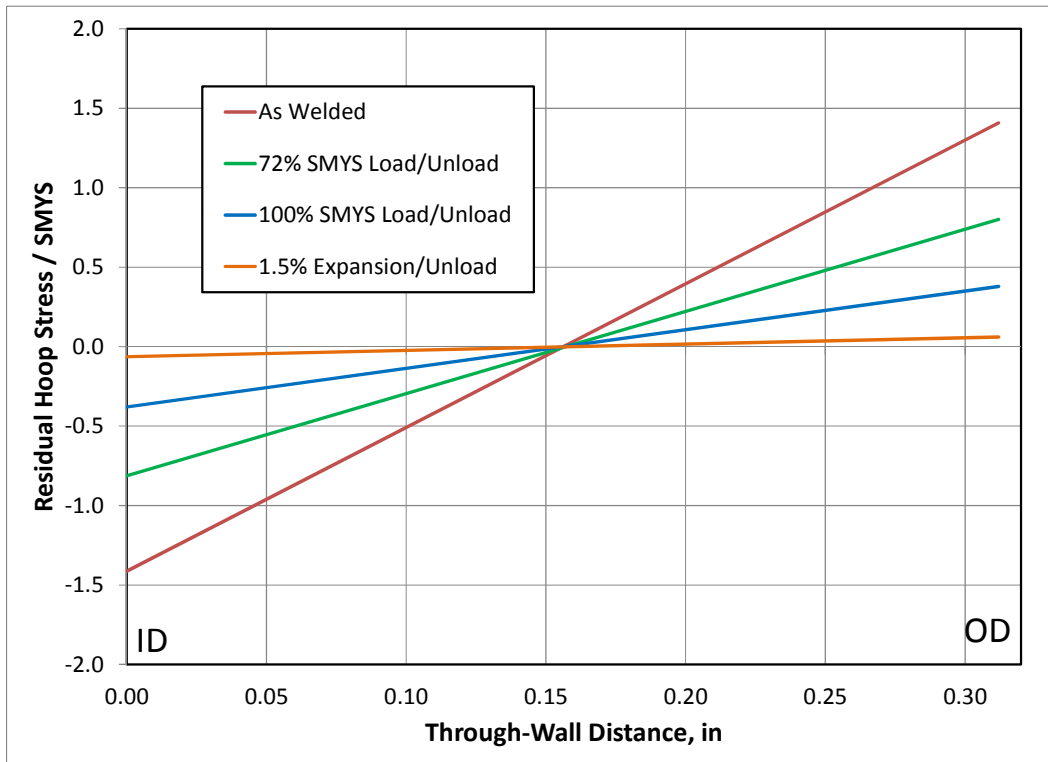


FIGURE 3. Linearized residual stress profiles, which were computed from the resultant through-wall bending moment.

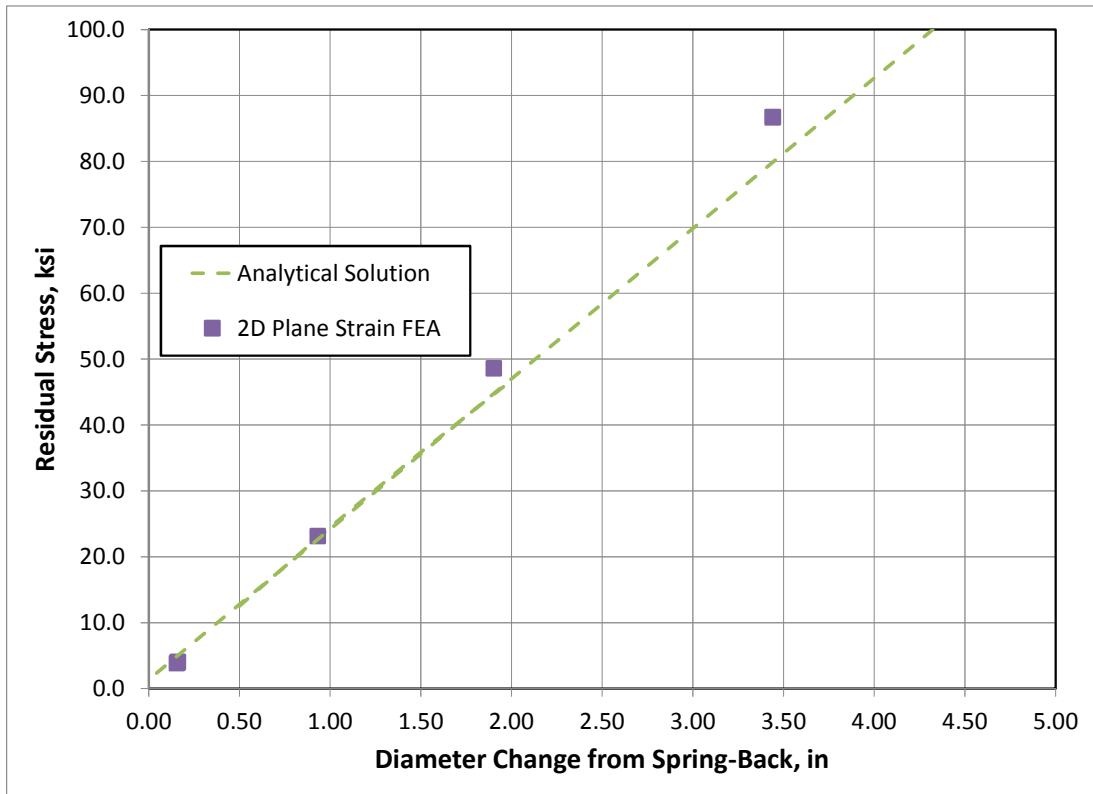


FIGURE 4. Relationship between residual stress and spring-back, as computed from FEA and Eq. [1].

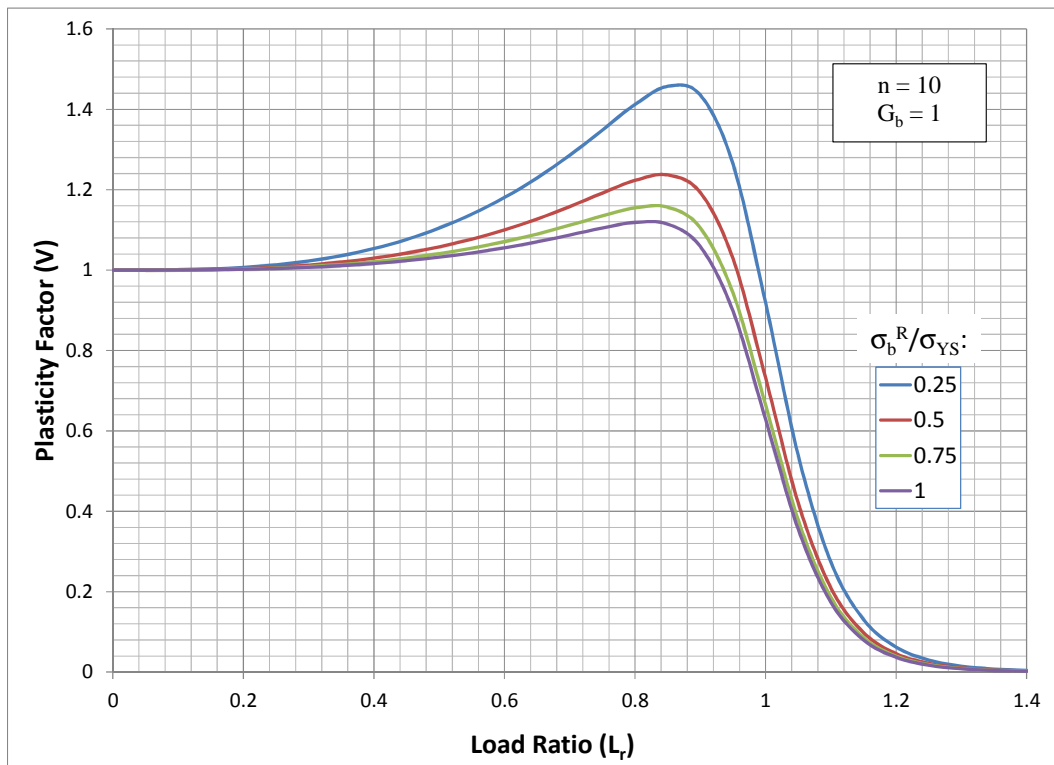


FIGURE 5. Plasticity correction factor on the elastic stress intensity factor due to residual stress (Eq. [4]).

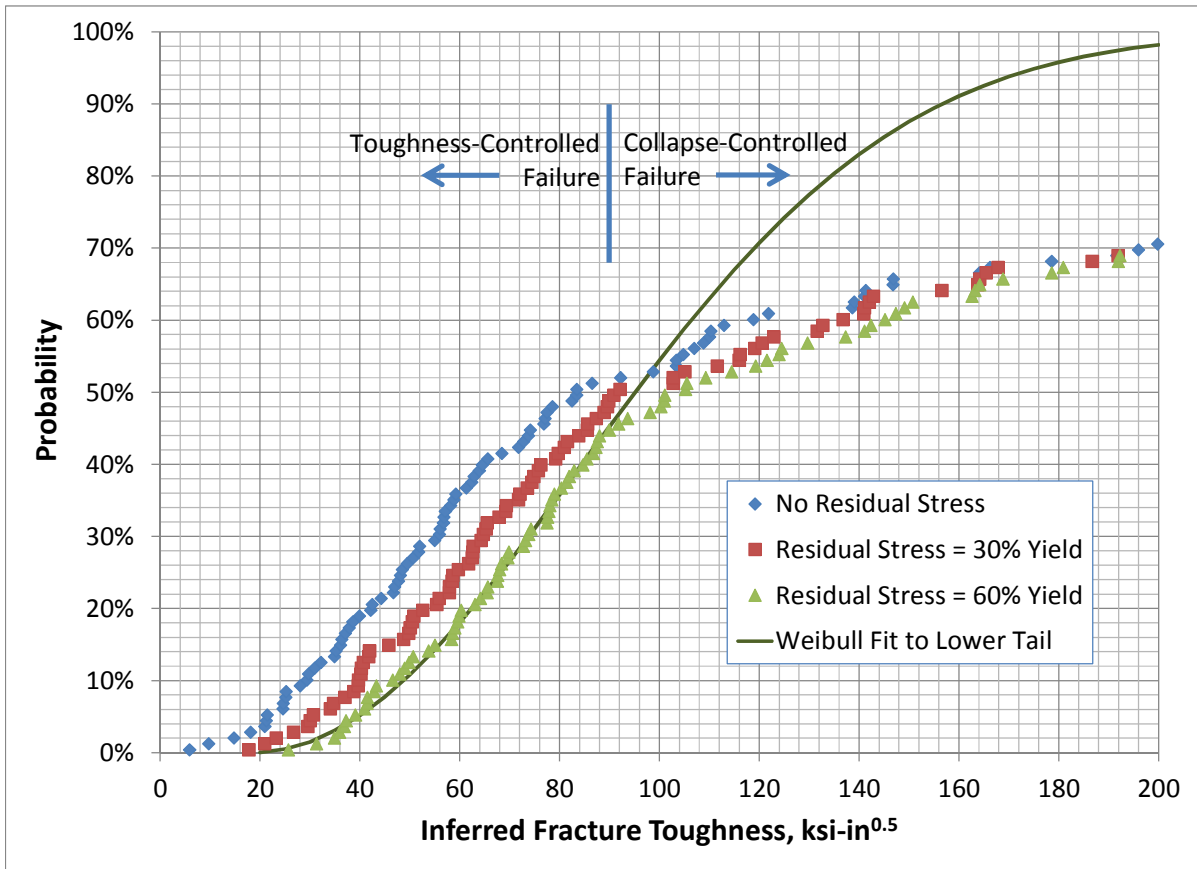


FIGURE 6. Fracture toughness inferred from 124 seam weld failures (4, 5), based on the modified MAT-8 fracture model.

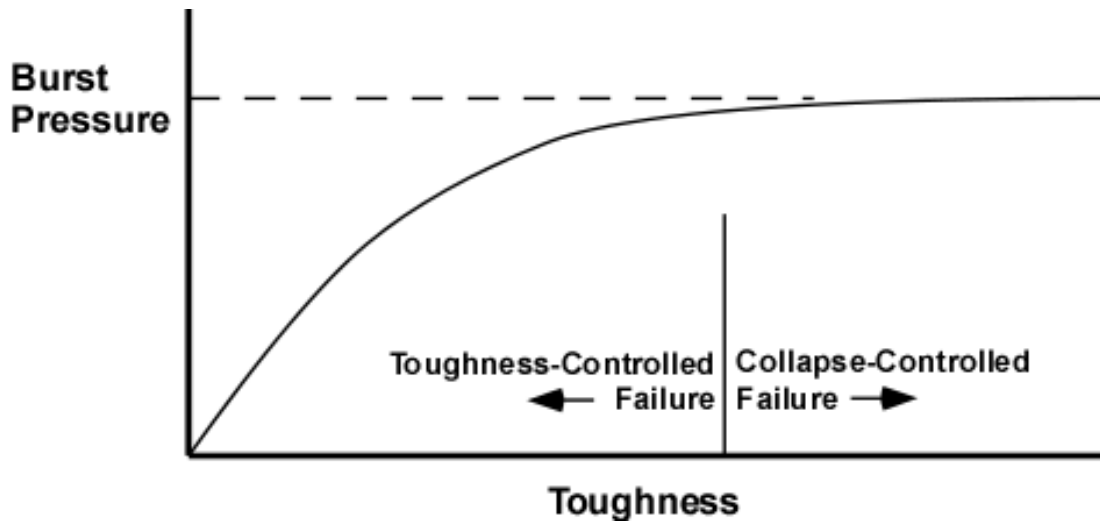


FIGURE 7. Relationship between burst pressure and toughness, given a particular flaw size.